arXiv:1210.3649v1 [cond-mat.mes-hall] 12 Oct 2012

Minimal self-contained quadridot quantum refrigeration machine

Davide Venturelli[1,2], Rosario Fazio[1], and Vittorio Giovannetti[1]
[1] *NEST, Scuola Normale Superiore and Istituto Nanoscienze-CNR, Piazza dei Cavalieri 7, I-56127 Pisa, Italy,*
[2] *Quantum Computing Laboratory, USRA, NASA Ames Research Center, Moffett Field CA 94035-1000.*
(Dated: October 16, 2012)

We present a theoretical study of an electronic quantum refrigerator based on four quantum dots arranged in a square configuration, in contact with as many thermal reservoirs. We show that the system implements the basic minimal mechanism for acting as a self-contained quantum refrigerator, by demonstrating heat extraction from the coldest reservoir and the cooling of the nearby quantum-dot.

PACS numbers: 03.65.Yz, 03.67.-a, 73.63.Kv, 73.23.-b

The increasing interest in quantum thermal machines has its roots in the need to understand the deep relations between thermodynamics and quantum mechanics [1, 2]. The progress in this field may as well have important applications in the control of heat transport in nano-devices [3]. In a series of very interesting works [4–6] the fundamental limits to the dimensions of a quantum refrigerator have been found. It has further demonstrated that these few-level quantum machines could still attain Carnot-efficiency [5] thus launching the call to find physical implementations of the smallest possible quantum refrigerator. Refs.[4–6] considered self-contained thermal machines defined as those thermal machines that perform a cycle without the supply of external work. Their action being grounded on the steady-state heat transfer from thermal reservoirs maintained at different temperatures. While such devices are ordinary in the macroscopic world, their realization in the quantum realm is challenging.

As recognized in recent works [7, 8] on self-contained refrigerators (SCR) the major difficulty in the realization of the three-qubits quantum machines of [4, 5] is the engineering of the crucial three-body interaction enabling the elastic transition between a doubly excited state in contact with a hot (H) and cold (C) reservoir, and a singly-excited state coupled to an intermediate-temperature (or "room-temperature" - R) bath. In this paper we get around this problem by proposing an experimentally feasible implementation of a minimal quantum refrigerator in a small array of semiconducting quantum dots (see Fig. 1) operating in the Coulomb blockade regime. With this work we are thus able to establish a further connection between the general theory of quantum thermal machines and the heat transport in nanoelectronics [3].

QDs contacted by leads have been recognized as prototypical systems for achieving high thermopower, see [9–11] and references therein, or anomalous thermal effects [12]. Here we study a four-QD planar array (hereafter named a "quadridot" for simplicity) coupled to four independent electron reservoirs as shown in Fig. 1; with proper (but realistic) tuning of the parameters, we will show that this system can effectively represent an implementation of the model described in Ref. [4]. Specifically we will show that the quadridot acts as a refrigerator which pumps energy *from* the high temperature reservoir H and the low temperature reservoir C *to* the intermediate temperature reservoirs R$_1$, R$_2$. Furthermore we will analyze the conditions under which the quadridot is able to cool the quantum dot QD_c which is directly connected to the bath C, at an effective temperature that is lower than the one it will have in the absence of the other reservoirs. This will lead us to introduce an operative definition of the local effective temperature depending on the measurement setup, and to predict the existence of intermediate working regimes where, for instance, the refrigeration is not accompanied by the cooling of QD_c. In deriving our results we start from a detailed analy-

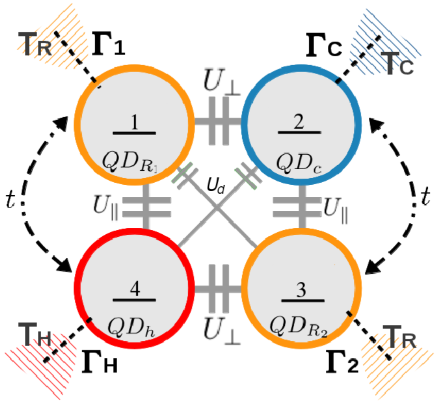

FIG. 1: [Color online] The quadridot. Vertical and Horizontal interdot capacitances are considered to be the highest energy scales among those in the figure. Their values $U_\parallel$ and $U_\perp$ are determined by the arrangement of the top gates over the QDs, which are not shown. The four quantum dots QC_h, QC_c, QC_{R_1} are QC_{R_2} are weakly tunnel coupled to the electronic reservoirs H, C, R$_1$, and R$_2$, respectively, which are all grounded but maintained at equilibrium at a well-defined temperatures $T_H > (T_{R_1} = T_{R_2} = T_R) > T_C$. No tunneling is possible between dot 1 (orange) and dot 2 (blue), and between dot 4 (red) and dot 3 (orange). [See text for the definition of the other symbols].

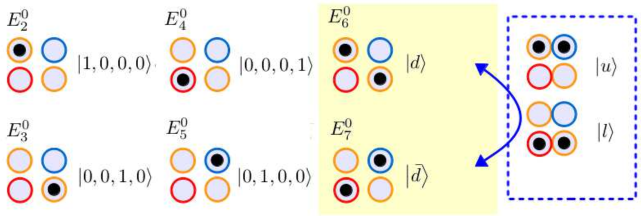

FIG. 2: [Color online] Pictorial view of the low-energy electronic charged states of the quadridot of Fig. 1 when it is isolated from the thermal reservoirs (a black circle inside the dot indicate that the latter is occupied by an electron. The completely empty state of energy $E_1^0 = 0$ is not shown). The indicated energies correspond to the $t = 0$ case. The two electron states $|d\rangle$ and $|\bar{d}\rangle$ are resonant, while $|u\rangle$ and $|l\rangle$ are the high-energy virtual states responsible for the effective coupling $g_{d\bar{d}}$ which couples them after the unitary transformation (see text). The remaining 7 high-energy states (2 two-particle states, 4 three-particle states and 1 fully occupied state) are not drawn as their contribution to the projected dynamics is negligible.

sis of the system Hamiltonian to identify the working regimes that allows us to mimics the behavior of the SCR of Ref. [4].

In the absence of the coupling to the leads, the array of QDs (the quadridot) shown in Fig. 1 is described by the Hamitonian

$$\mathcal{H}_{QD} = \sum_{i=1,4} \epsilon_i n_i + \sum_{i\neq j} U_{ij} n_i n_j - t(c_1^\dagger c_4 + c_2^\dagger c_3 + \text{h.c.}), \quad (1)$$

where $\epsilon_{1,\cdots,4}$ denote the single particle energy level of the dots, and where we introduced the creation/annihilation operators $c_i^\dagger$, c_i of an electron in the i-th dot and $n_i = c_i^\dagger c_i$. The matrix U_{ij} takes into account the finite-range contribution of the Coulomb repulsion while the parameter t gauges the tunneling coupling. The level separation in each dot is assumed to be large enough such that it is sufficient to consider only one level. Moreover the on-site repulsion is taken as the largest energy scale in the problem reducing the maximum occupancy in each to to one electron. Gates are applied to the dots in order to tune their single-electron energy level of the upper-right dot (which will be coupled to the cool resorvoir) to $\epsilon_2 = \epsilon_1 + \epsilon_3 - \epsilon_4$. We assume that $U_{12} = U_{34} = U_\perp$ and $U_{23} = U_{14} = U_\parallel$, both much larger than the diagonal term $U_{24} = U_{13} = U_d$. The charge states of our system are labeled according to the occupation of the four dots $|n_1, n_2, n_3, n_4\rangle$. The single electron level ϵ_2 is chosen so that in the absence of tunneling ($t = 0$), the "diagonal" two-particle states $|d\rangle = |1,0,1,0\rangle$ and $|\bar{d}\rangle = |0,1,0,1\rangle$ shown in Fig. 2 are, for $t = 0$, degenerate (in our model they play the role of the states $|01\rangle, |10\rangle$ of [4]).

Before going in the detailed description of the refrigerator, it is instructive to see what are the states that will play a leading role in the thermal cycle. The lowest energy subspace can be identified by the four states with single occupancy $|1\rangle = |1,0,0,0\rangle$, $|2\rangle = |0,1,0,0\rangle$, $|3\rangle = |0,0,1,0\rangle$, and $|4\rangle = |0,0,0,1\rangle$. In the two-electron sector only the states $|d\rangle$ and $|\bar{d}\rangle$ are relevant. The two other states $|u\rangle = |1,1,0,0\rangle$ and $|l\rangle = |0,0,1,1\rangle$ are much higher in energy, as they involve $U_\perp$ or $U_\parallel$. They however play a fundamental role in the refrigerator as they allow to generate and effective coupling between the states $|d\rangle$ and $|\bar{d}\rangle$. This can be see by performing a Schrieffer-Wolff transformation [13, 14]: one can show that besides a slight-renormalization of the single particles levels (which we will ignore), a direct coupling among $|d\rangle$ and $|\bar{d}\rangle$ emerges with an intensity which can be well-approximated by

$$g_{d\bar{d}} \simeq \frac{2t^2(U_d - U_\perp)}{(U_d - U_\perp)^2 - (\epsilon_4 - \epsilon_1)^2} \ll t. \quad (2)$$

In our model this is the analogous of the crucial perturbative g term discussed in Ref. [4] as it allows to perform a coherent swap between the state connected to the room-temperature reservoir ($|\bar{d}\rangle$) to the doubly occupied state $|d\rangle$ which is simultaneously in contact with the hot and cold bath. Due to the effective hoppings of t and $g_{d\bar{d}}$ the eigenstates of the low-energy Hamiltonian will be the bonding-antibonding states $|d\rangle \pm |\bar{d}\rangle$ and the four bonding-antibonding single particles states delocalized between the dots 1, 4 and 2, 3.

As anticipated, each QD is contacted to an independent electron reservoir characterized by a chemical potential μ_i and temperature T_i, appearing in the Fermi-Dirac occupation functions $f_i(\epsilon)$. For the sake of the simplest correspondence with the model of Ref. [4] in this study all μ_i will be set to be identical and fixed to a value that will be used as reference for the single particle energies of the system [e.g. setting $\epsilon_i = 0$ in Eq. (1) corresponds to have the i-th quadridot level at resonance with the Fermi energy of the reservoirs]. Furthermore the temperatures will be chosen as $T_1 = T_3 = T_R$, $T_C = T_2$ and $T_H = T_4$ satisfy $T_C < T_R < T_H$ for the refrigerator to work [15] [the change in the notation helps in identifying the cool, hot and room temperature reservoirs]. Within these assumptions, the only required external action is exerted in maintaining the local equilibrium temperatures and chemical potential, in accordance to the standard definition of self-containance. The equilibrium correlation functions ($a_{i,k}/a_{i,k}^\dagger/$ destroys/creates an electron in lead i and momentum k) read $\sum_k \int e^{i\epsilon t} \langle a_{i,k}^\dagger(t) a_{i,k}(0)\rangle dt = f_i(\epsilon)\nu_i(\epsilon)$ and $\sum_k \int e^{i\epsilon t} \langle a_{i,k}(t) a_{i,k}^\dagger(0)\rangle dt = (1 - f_i(\epsilon))\nu_i(\epsilon)$. In the previous expression $\nu(\epsilon)$ is the local density of states of the lead [16]. The coupling to the leads (parametrized by the amplitudes $\Gamma_i^{(k)}$) reads

$$H_T = \sum_{i=1,4} \sum_k \Gamma_i^{(k)} c_i^\dagger a_{i,k} + \text{h.c.} \quad (3)$$

giving rise, in the Born-Markov-Secular limit [17, 18], to

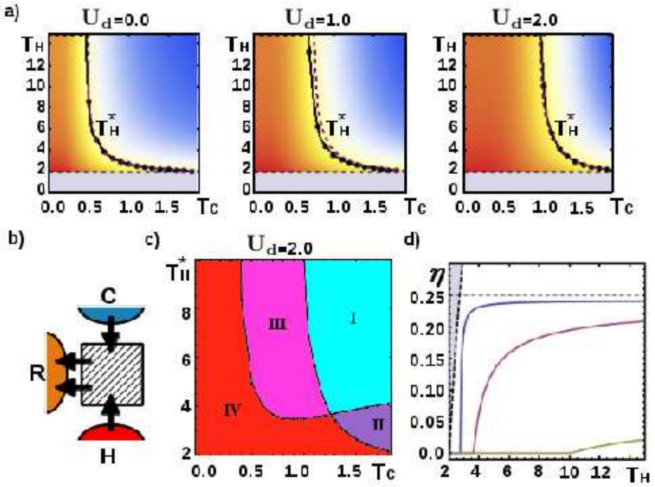

FIG. 3: [Color online] a) Working conditions of the refrigerator. Panels refer to $U_d = 0$ (left), $U_d = 1$ (center), $U_d = 2$ (right). The change of sign in the heat flow occurs at T_H^* at a value very close to the analytical value of Eq. (6) (dashed line). For $T_H > T_H^*$ (blue region) machine works as pictured in b), extracting heat from the C,H-reservoirs and pumping it into R. Black dashed line above the grey region indicates $T_H = T_R$=2. Blue/Red background color intensity is proportional to the actual heat pumped to/extracted from C-reservoir. c) Possible temperature regimes for $U_d = 2$. In regions I/II the refrigerator is working (heat is extracted from C) while in regions III/IV the C bath *receives* heat. In regions I/III we have an effective decrease of single particle occupation number (i.e. $\mathbf{n}_C < \mathbf{n}_C^0$). d) Efficiency of the refrigerator compared to the Carnot efficiency (dashed black line) for T_C=1.0. The curves represents $U_d = 0$ (blue), $U_d = 1$ (magenta) and $U_d = 2$ (brown). The dashed horizontal line indicates maximum limit of efficiency for the quadridot computed (for $U_d = 0$) as in [4].

a Lindblad master equation for the reduced density matrix ρ of the quadridot. The presence of t plus the unitary rotation into the low-energy sector eliminates any degeneracy between all possible energy transitions between the eigenstates of the quadridot. The evolution of ρ is then determined by the master equation

$$\dot{\rho} = \sum_i \mathcal{D}_i\left[\rho\right] \ , \tag{4}$$

where for each reservoir $\mathcal{D}_i$ represents associated Lindblad dissipator. This equation can be solved in the steady-state regime ($\dot{\rho} = 0$) yielding the asymptotic configuration ρ^∞, from which the heat currents $\langle \mathbf{J}_{Q,i} \rangle$ flowing through the i-th reservoir are then easily computed as [17],

$$\langle \mathbf{J}_{Q,i} \rangle \ = \ \mathrm{Tr}\Big[\mathcal{H}_{QD}\ \mathcal{D}_i\left[\rho^\infty\right]\Big] \ . \tag{5}$$

If the correspondence between our device and the theoretical qubit model of [4] is correct, we should see a direct heat flow *from* the hot and cold reservoirs *to* the room temperature reservoirs, while dot coupled to the cold reservoir should reach an occupation probability lower, $\epsilon_2 > 0$ than the one dictated by its local reservoir (See Fig. 3-b). We have verified this by setting the system parameters to be consistent with those presented in Ref. [4] (making sure however that for such choice no additional degeneracies are introduced into the system due to the larger dimension of our physical model). For this reason we choose $\epsilon_1 = 2.1$, $\epsilon_3 = 2.9$, $\epsilon_4 = 4.0$, $\Gamma_i = 0.001$ (momentum independent [16], $U_\perp = 12.0$, while kept $U_\parallel = \infty$ for simplicity as its effect could be absorbed in the energy level renormalization after the Schrieffer-Wolff transformation. The value of $g_{d\bar{d}}$ is then fixed to be -0.001 determining t ($\lesssim 0.1$) through Eq. (2) (in all these expressions the energy units should be considered as multiples of 100 μeV in order to be experimentally reasonable). Solving numerically the steady state equation (4) we then notice that for each $T_C < T_R$, there exists a minimal threshold T_H^* for T_H above which the refrigerator indeed extracts heat from the cold reservoir C. The results are plotted in Fig. 3-a for T_R=2 and different values of U_d: notice that consistently with the second principle of thermodynamics T_H^* is always greater than $T_R = 2$ (for T_H below T_R the machine cannot produce work from H to pump heat from C), and that the functioning region $T_H \geq T_H^*$ gets larger as U_d gets smaller. The existence of the threshold T_H^* implies also that, for given $T_H > T_R$, there is a minimal temperature T_C^* for the cold reservoir under which the refrigerator cannot work. Interestingly enough for $T_H/T_R \to \infty$ the value of T_C^* appears to asymptotically converge toward a finite non-zero temperature $\bar{T}_C^*$ which depends upon the engine microscopic parameters and which can be interpreted as *the emergent absolute zero* of the model. An approximate analytical expression for T_C^* (and hence T_H^*) can be derived exploiting the recent general theory of genuine, maximally-efficient self-contained quantum thermal machines [6]. This is done by interpreting the quadridot as a composite system, consisting of the QD_c at equilibrium with its local reservoir, in contact (by means of $g_{d\bar{d}}$) with an "effective" virtual qubit whose states are defined by $|0,0,1,0\rangle$ and $|d\rangle$ (See Fig. 2) and whose average occupation is determined by a virtual temperature that can be interpreted as our T_C^*. Following [6] this yields the expressions

$$T_C^* \simeq T_R T_H \tfrac{\epsilon_1+\epsilon_3-\epsilon_4+U_d}{T_H(\epsilon_1+\epsilon_3+U_d)+T_R\epsilon_4}, \quad \bar{T}_C^* \simeq T_R(1-\kappa), \tag{6}$$

with $\kappa = \epsilon_4/[\epsilon_1 + \epsilon_3 + U_d]$, which fit pretty well our numerical results (See Fig. 3-a) [19].

Following [5], we also evaluate the ratio $\eta = \langle \mathbf{J}_{Q,2} \rangle / \langle \mathbf{J}_{Q,4} \rangle$ between the heat current through the cold and hot reservoirs comparing it with the upper bound $(1 - \frac{T_R}{T_H})/(\frac{T_R}{T_C} - 1)$ posed by the Carnot limit, and with the theoretical value of the three-qubit model [4] applied to the quadridot for $U_d = 0$ [20], η_{th}=$(\epsilon_1 + \epsilon_3 - \epsilon_4)/\epsilon_4$. The dependence of η as a function of T_H are plotted in Fig. 3-d for different values of U_d. We noticed that in the special case U_d=0 the efficiency of the quadridot converges indeed towards the theoretical value η_{th} of [4] at least for large enough T_H.

Effective Local Temperatures:– The sign of the heat flow in the working region suggests that any object (defined by a local Hamiltonian) interposed between the QD_2 and its bath will necessarily be cooled by the SCR. An important question is whether this refrigeration effect is accompanied with a cooling of the interacting QD_c, namely whether its effective local temperature $T_C^{(eff)}$ decreases as T_H increases, for sufficiently high T_H, in analogy with the qubit-cooling described in Ref. [4]. While for such idealized qubit model the definition of the local temperature is relatively straightforward, in nanoscale systems out of equilibrium, local temperatures must be *operationally* defined [21]. A natural way to proceed is to introduce a probe reservoir P (a "thermometer") which is weakly coupled to that part of the system we are interested in (the dot QD_c in our case) and identify the effective temperature of the latter with the value of the temperature T_P of the probe which nullifies the heat flow through P. This procedure can be implemented easily in our model by adding an extra term in (3) that connects the new reservoir P to QD_c with a tunnel amplitude Γ_P which is much smaller than those associated with the other reservoirs of the system (in the calculation we set the ratio between Γ_P and $\Gamma_{C,T,R}$ to be of the order 10^{-3}: this make sure that the presence of P does not perturb the system). The obtained values of $T_C^{(eff)}$ are presented in Fig. 3-a where it is shown that, according to this definition of the local temperature, the conditions for cooling of QD_c (i.e. $T_C^{(eff)} < T_C$) are the same for the refrigerator to work (in particular this implies $T_C^{(eff)}$ is always greater than the emergent zero-temperature of the system).

The quantity $T_C^{(eff)}$ introduced above has a clear operational meaning and it is our best candidate to define the effective temperature of QD_c. Still it is important to acknowledge that in experiments the cooling of QD_c could also be detected by looking at the decrease of the mean asymptotic occupation number of the QD_c (i.e. $\langle \mathbf{n}_C \rangle = \langle 0,1,0,0|\rho^\infty|0,1,0,0\rangle + \langle d|\rho^\infty|d\rangle$), with respect to the same quantity computed when the refrigerator is "turned off" (e.g. $\langle \mathbf{n}_C^0 \rangle = \langle 0,1,0,0|\rho_0^\infty|0,1,0,0\rangle + \langle d|\rho_0^\infty|d\rangle$ where now ρ_0^∞ is the asymptotic stationary state of the system reached when all the reservoirs but C are disconnected, i.e. $\Gamma_H = \Gamma_{R_1} = \Gamma_{R_2} = 0$). We notice however that the cooling condition hereby defined does not coincide with the same pictured in Fig. 3-a. We indeed exemplify in Fig. 3-c for U_d=3 that according to this new definition of cooling different operating regimes are generally possible for the refrigerator. The QD_c might be either colder ($\mathbf{n}_C < \mathbf{n}_C^0$ in zone I) or hotter ($\mathbf{n}_C > \mathbf{n}_C^0$, in region II) when the device extract heat from the C reservoir. Conversely, we might achieve a colder QD_c also when the quadridot pumps heat into the colder bath (III). For the temperatures region IV none of the refrigeration effects is active. For completeness, we also report that the effective local temperatures of the other three QDs are generally positively correlated with the increase of T_H, witnessing the intuitive consideration that cooling of one part of the quadridot is made at the expenses of the heating of the rest of the device, independently from the operational definition of local temperature. Similar intermediate regimes emerge with other activation prescriptions, such as defining $\langle \mathbf{n}_C^0 \rangle$ as the occupation for $T_H = T_R = T_C$ while maintaining all tunnel couplings as constant.

Conclusions:– We conclude by commenting on the possibility of experimentally attaining the physical regimes described in the manuscript. Quadridots in standard GaAs/AlGaAs heterostructures have been implemented aiming at Cellular-Automata computation [22] and very recently for controlled single-electron manipulation [23]. Strongly capacitively-coupled QDs with interdot capacitance energy ($U_\perp$ and $U_\parallel$) up to 1/3 of the intra-dot charging energy (taken to be infinite in our model) can be fabricated with current lithographic techniques [24]. The diagonal inter-dot term U_d is expected to be at most $U_\parallel/\sqrt{2} \simeq U_\perp/\sqrt{2}$ from geometrical considerations, but practically it is expected to be much smaller [23] and in principle can be reduced arbitrarily with appropriate dielectrics or by sputtering in the center of the quadridot. Experimentally, the local charging energy can be as big as 1 meV, and usually represents about 20% of the confinement energy [25], which is the typical tunable values of the single-particles levels ϵ_i. While these ratios can already partially justify the spectral scales necessary for the refrigerator to work, charging effects (relative to single-particles levels) are expected to be further enhanced by the presence of a significant magnetic field, due to the emergence of the incompressible antidot regime in the dots [26], possibly allowing the necessary working conditions to be achieved more easily. We also note that in this high-field regime, the spin/orbital-Kondo effect (which is expected active in these kind of devices [27, 28]) is suppressed [29], as the transport becomes spin-polarized, so our effective description is expected to be valid. We finally note that the maximum thermal energies involved should not exceed the large charging energies, so the bath temperatures should all be $\lesssim$ 10K.

We acknowledge useful discussions with C. W. J. Beenakker and support from MIUR through the FIRB-IDEAS project RBID08B3FM, by EU through the Project IP-SOLID, and by KK9.

---

[1] G. Gemma, M. Michel and G. Mahler, *Quantum Thermodynamics*, Springer (Berlin, 2004).

[2] K. Maruyama, F. Nori, and V. Vedral, Rev. Mod. Phys. **81**, 1 (2009); M. Esposito, H. Harbola, and S. Mukamel, Rev. Mod. Phys. 81, 1665 (2009).

[3] F. Giazotto, T. T. Heikkilä, A. Luukanen, A. M. Savin, and J. P. Pekola, Rev. Mod. Phys. **78**, 217 (2006).

[4] N. Linden, S. Popescu, and P. Skrzypczyk, Phys. Rev. Lett. **105**, 130401 (2010).

[5] P. Skrzypczyk, N. Brunner, N. Linden, and S. Popescu, J. Phys. A Math. Theor. **44**, 492002 (2011).

[6] N. Brunner, N. Linden, S. Popescu, and P. Skrzypczyk, Phys. Rev. E **85**, 051117 (2012).

[7] Y. Chen, and S. Li, Europhys. Lett. **97**, 40003 (2012).

[8] A. Levy and R. Kosloff, Phys. Rev. Lett. **108**, 070604 (2012).

[9] C. W. J. Beenakker and A. A. M. Staring, Phys. Rev. B **46**, 9667 (1992).

[10] D. Bose and R. Fazio, Europhys. Lett. **56**, 576 (2001).

[11] P. Trocha and J. Barnaś, Phys. Rev. B **85**, 085408 (2012).

[12] R. Sánchez, R. López, D. Sánchez, and M. Büttiker, Phys. Rev. Lett. **104**, 076801 (2010); R. Sánchez and M. Bütiker, Phys. Rev. B **83**, 085428 (2011).

[13] J. R. Schrieffer and P. A. Wolff, Phys. Rev. **149**, 491 (1966).

[14] S. Bravyi, D. P. DiVincenzo, and D. Loss, Annals of Physics **326**, 2793 (2011).

[15] Having set $T_{R_1} = T_{R_2}$ the reservoirs 1 and 2 can be considered a single incoherent reservoir: this hypothesis is not strictly necessary but it helps in simplifying the analysis.

[16] As discussed in Ref. [12], the energy dependence of the local density of states and the tunneling amplitudes in contacted QDs alone can be the origin of interesting thermal effects. While this additional degree-of-freedom may perhaps be used to shape the working regions of the SCR, we consider for simplicity these energy dependence to be negliglibly varying over the ranges of our energy splitting.

[17] H.P. Breuer and F. Petruccione, *The Theory of Open Quantum Systems* (Oxford University Press, Oxford 2002).

[18] G. Schaller, Course Lecture Notes "Non-Equilibrium Master Equations" (2012) and G. Schaller, G. Kie?lich, and T. Brandes, Phys. Rev. B **80**, 245107 (2009)

[19] It is worth observing that the working regimes of Fig. 3-a admits an interpretation within the virtual temperature model of Ref. [6]. Indeed when T_C is greater than the virtual temperature (6) then a heat flow from the C-reservoir towards the composite system represented by the virtual qubit is expected leading to refrigeration.

[20] Not null values of the parameter U_d introduce Coulomb interactions among degenerate resonant states which tend to spoil the correspondence with the three qubit system of Ref. [4]. For the model under consideration however it is not realistic to assume $U_d = 0$ so we keep it small but not null. It turns out that the performances of the system are not significantly affected by this choice (e.g. see Fig. 3).

[21] H. L. Engquist and P. W. Anderson, Phys. Rev. B **24**, 1151 (1981).

[22] F. Perez-Martinez, *et al.* Appl. Phys. Lett. **91**, 032102 (2007).

[23] R. Thalineau, S. Hermelin, A. D. Wieck, C. Bäuerle, L. Saminadayar, and T. Meunier, Appl. Phys. Lett. 101, 103102 (2012).

[24] I. H. Chan, R. M. Westervelt, K. D. Maranowski, and A. C. Gossard, Appl. Phys. Lett. **80**, 1818 (2002).

[25] A. Hübel, J. Weis, W. Dietsche, and K. v. Klitzing, Appl. Phys. Lett. 91, 102101 (2007).

[26] H. van Houten, C. W. J. Beenakker, and A. A. M. Staring, *Single Charge Tunneling*, edited by H. Grabert and M. H. Devoret, NATO ASI Series B, Vol. 294, (Plenum Press, New York, 1992).

[27] L. Borda, *et al.* Phys. Rev. Lett. **90**, 026602 (2003).

[28] D. E. Liu, S. Chandrasekharan, and H. U. Baranger, Phys. Rev. Lett. **105**, 256801 (2010).

[29] Y. Meir, N. S. Wingreen, and P. A. Lee, Phys. Rev. Lett. **70**, 2601 (1993).